Design of compact UWB antenna based on FSSIR feeder

MARYAM S. JAMEEL[1], YAQEEN S. MEZAAL[2,*], DOGU CAGDAS ATILLA[1]
[1]*Department of Electrical and Computer Engineering, Altinbas University, Istanbul, Turkey*
[2]*Department of Medical Instrumentation Engineering, Al-Esraa University College, Baghdad, Iraq*

This study describes a new ultra-wideband slotted patch antenna. The antenna is mounted on an FR-4 substrate with a size of 27.2×14×1.5 mm^3 and a permittivity of 4.3. A slotted patch resonator, four-stage stepped impedance resonators (FSSIR) feeder, and a reduced ground plane are features of our new antenna design. The input reflection values are 31, 30, and 32 dB at resonant frequencies of 3.3, 5.75, and 7.1 GHz, respectively, with a bandwidth range of 2.91–9.13 GHz, as determined by the simulated S11 response. The antenna was designed using the CST Microwave Studio simulator. The consequences of S11 simulations and actual measurements coincide rather well.

(Received August 19, 2022; accepted February 6, 2023)

Keywords: Microstrip, UWB, Slotted patch radiator, Reduced ground plane, FSSIR feeder

1. Introduction

Electromagnetic waves' transmission and reception are made possible by the antenna, which is a critical component of modern wireless communications [1]. An antenna is also considered a metallic transducer for transferring and receiving electromagnetic waves. A wide variety of antennas may be found in a wide variety of places, including private residences and public places like police stations, firehouses, schools, and even military installations. Originally, television antennas were designed to pick up broadcast signals that ranged in frequency from 41 MHz to 250 MHz in the ultra-high frequency band and 470 MHz to 960 MHz in the very high-frequency region [2]. Ultra-wideband (UWB) technology has received a lot of interest in the recent two decades from both academia and industry. UWB is a short-range, high-information spread across a comprehensive bandwidth technology that employs a very low energy level. Because of their short pulse durations, a high data rate and low latency may be achieved more easily with UWB pulses. This promotes the use of UWB in sensor networks, wireless positioning systems, biomedical imaging, and high-data-rate short-range communications. For UWB communication systems to work at their best, antennas must fulfill a wide range of characteristics, including impedance matching, good radiation patterns, small size, and cost-effectiveness. UWB applications benefit from the patch antenna, which is lightweight and straightforward for other electrical components to be integrated [3]. There is always the possibility of interference signals affecting UWB systems. UWB antennas may be designed with band-notched features to overcome interference signals [4].

Additionally, UWB systems can operate in short- and long-range frequency spectrums and high data rates with cheap production costs. It is also possible to utilize a single UWB antenna instead of many smaller antennas. Due to its ease of integration with Monolithic Microwave Integrated Circuits, the microstrip patch antenna design is now prevalent in communication devices [5]. UWB communication applications are many, but Low Data Rate (LDR) transmitters are simple transmitters that limit the unnecessary use of energy, thereby allowing the battery to survive longer. UWB pulses generally have a very short range, often a few nanoseconds; hence the frequency spectrum is ultra-wideband. Low-information-rate systems, such as those used by the military services, rely heavily on this technique since it is difficult to recognize and infrequently up to blocking security. Besides that, UWB is also used in applications requiring high data rates, such as random number generators, access to online and mixed media services, area-specific services, home management systems, and gadgets [6]. The bandwidth of the slotted microstrip patch antenna is limited. The antenna's bandwidth can be increased by using several slots in addition to the primary slot [7]. Since the multi-standard wireless system requires the resonator to perform at several frequencies, a paradigm change in resonator design is needed.

In low-power applications, planar resonators are critical. The narrow bandwidth of Q resonators made them desirable for oscillators and filters because of their high price. Uniform Impedance Resonator (UIR) is the simplest resonator, while Stepped Impedance Resonator (SIR) is the appropriate extension. Over the last several decades, SIR has established itself as a viable alternative to UIR in the design of planar circuits and has shown to be an effective filtering method. Makimoto and Yamashita were the first to develop SIR in the 1980s. SIR is the most intriguing characteristic designed to shift the higher spurious bands without affecting the fundamental frequency while simultaneously operating in several bands. Over the years, designers have contended with the increased demand for multimode wireless systems, which has imposed additional constraints. As a consequence of the design changes, a variety of resonators are now

available. To minimize the size of the circuit, SIRs might be utilized [8]. Shorter SIRs have a lower impedance ratio, which means a shorter overall length. Changing the impedance and length ratio [9] allows them to simultaneously produce spurious responses at higher frequencies. A new type of UWB-based microstrip antenna has been proposed in [10]. Specifically, a rectangular radiator patch with dual L-shaped slots has been developed to increase the current path to both sides of the radiating patch. In addition, a two-step impedance resonator structure was added at one end of the radiation patch and the antenna feeder to achieve a broadband impedance bandwidth from 2.39 GHz to 13.78 GHz.

This work aims to develop a microstrip antenna with extreme compactness and ultra-wideband operation. The slotted patch resonator, partial ground plane, and stepped-impedance resonators were employed in antenna design using a single-layer FR4 substrate. This study has revealed that the antenna's impedance bandwidth and input reflection have been enhanced by employing four-stage stepped-impedance resonators and one customized reduced ground unit.

2. Four-stage stepped impedance resonators (FSSIR)

For the designed UWB-antenna in this study, the FSSIR structure, properties, and equations are depicted in this section. The characteristic impedances Z1, Z2, Z3, and Z4 are included for FSSIR, while the four stages' electrical lengths are represented by 1, 2, 3, and 4. Unlike two- and three-section SIRs, the proposed FSSIR offers at least four degrees of freedom for flexible regulation of the first four resonant frequencies. Since FSSIR is symmetrical, both even-mode and odd-mode techniques can be used to extract its resonant characteristics; its odd-mode and even-mode equivalent circuits are depicted in Figs. 1B and C, respectively. Here is how to determine Z1234odd and Z1234even from Figs. 1B and 1 [11, 12].

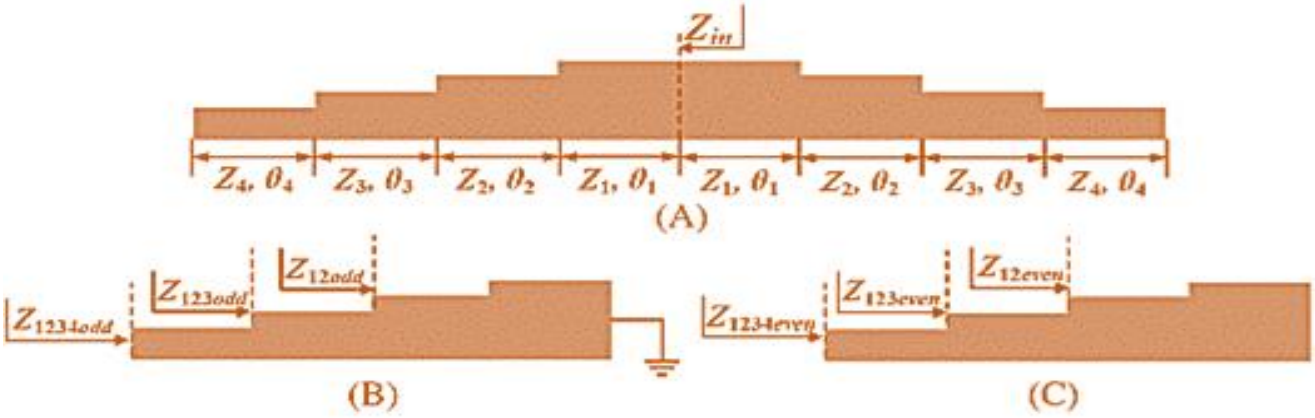

Fig. 1. Configuration and equivalent circuits of the proposed four-stage stepped-impedance resonator (FSSIR). A, Configuration. B, Odd-mode equivalent circuit. C, Even-mode equivalent circuit

$$z_{1234odd} = z_4 \frac{z_{123odd} + jz_4 \tan\theta_4}{z_4 + jz_{123odd} \tan\theta_4}$$

where

$$z_{123odd} = z_3 \frac{z_{12odd} + jz_3 \tan\theta_3}{z_3 + jz_{12odd} \tan\theta_3}$$

where

$$z_{12odd} = jz_2 \frac{z_1 \tan\theta_1 + z_2 \tan\theta_2}{z_2 - z_1 \tan\theta_1 \tan\theta_2}$$

Even mode

$$z_{1234even} = z_4 \frac{z_{123even} + jz_4 \tan\theta_4}{z_4 + jz_{123even} \tan\theta_4}$$

where

$$z_{123even} = z_3 \frac{z_{12even} + jz_3 \tan\theta_3}{z_3 + jz_{12even} \tan\theta_3}$$

$$z_{12even} = jz_2 \frac{-z_1 \cot\theta_1 + z_2 \tan\theta_2}{z_2 + z_1 \cot\theta_1 \tan\theta_2}$$

For simplicity, let $\theta = \theta1 = \theta2 = \theta3 = \theta4$ and $0 < \theta \leq \pi/2$. When $Y_{1234odd} = {}^{1}/_{Z_{1234odd}} = 0$ and $Y_{1234even} = {}^{1}/_{Z_{1234even}} = 0$, the resonant conditions can be acquired. If we define K2 = Z2/Z1, K3 = Z3/Z1, and K4 = Z4/Z1, then, as $\theta \neq {}^{\pi}/_{2}$ the resonant conditions can be modified as below:

$$K_3^2 tan^4\theta - (K_2K_30 + k_2^2K_3 + K_2K_3^2 + K_2K_4 + K_2^2K_4 + K_3K_4)\tan^2\theta + k_2K_3K_4 = 0$$

For even mode:

$$K_2K_3K_4 + K_2K_3 + K_2K_4 + K_3K_4 - (K_2K_3^2 + K_2^2K_4 + K_3^2)tan^2\theta = 0$$

By solving the above equations, the resonant conditions are feasibly presumed as odd mode:

$$\theta = \begin{cases} arctan\sqrt{\dfrac{M+\sqrt{M^2}-4K_2K_3^3K4}{2K_3^2}} \\ arctan\sqrt{\dfrac{M-\sqrt{M^2}-4K_2K_3^3K4}{2K_3^2}} \end{cases}$$

$$M = K_2K_3 + K_2K_4 + K_3K_4 + K_2^2K_3 + K_2^2K_4 + K_3^2K_2$$

For even mode,

$$\theta = \sqrt{\frac{K_2K_3K_4 + K_2K_3 + K_2K_4 + K_3K_4}{K_2^2K_3 + K_2^2K_4 + K_3^2K_2 + K_3^2}}$$

As $\theta = \pi/2$, then it is alternative solution for resonant condition of even mode. If the initial four resonant frequencies for proposed FSSIR are symbolized as f1, f2, f3, f4, where f1 and f3 are excited by odd mode, while f2 and f4 are excited by even mode, then:

$$\frac{f_1}{f_4} = \frac{arctan\sqrt{M-\sqrt{\dfrac{M^2-4K_2K_3^3K_4}{2K_3^2}}}}{\pi/2}$$

$$\frac{f_2}{f_4} = arctan\sqrt{\frac{K_2K_3K_4 + K_2K_3 + K_2K_4 + K_3K_4}{K_2^2K_3 + K_2^2K_4 + K_3^2K_2 + K_3^2}} \Big/ \frac{\pi}{2}$$

$$\frac{f_3}{f_4} = \frac{arctan\sqrt{M+\sqrt{\dfrac{M^2-4K_2K_3^3K_4}{2K_3^2}}}}{\pi/2}$$

The above equations can be used to determine the unique set of solutions for the four operating frequencies. Subsequently, the impedances of Z1 to $Z4$ may then be calculated. In addition, the impedance may be used to alter the frequency ratios f1/f4, f2/f4, and f3/f4 in various ways. Fig. 2 shows that f3/f4 fluctuates against the K2 substantially more than f1/f4 and f2/f4. This means that adjusting K2 allows for separate control of f3/f4. Additionally, with the increase of K3, f1/f4 mostly keeps unaltered, whereas f2/f4 and f3/f4 differs with the same extent. The results indicate that K3 has the ability to regulate f2/f4 and f3/f4. In addition, the three frequency ratios are all seen to rise as K4 increases.

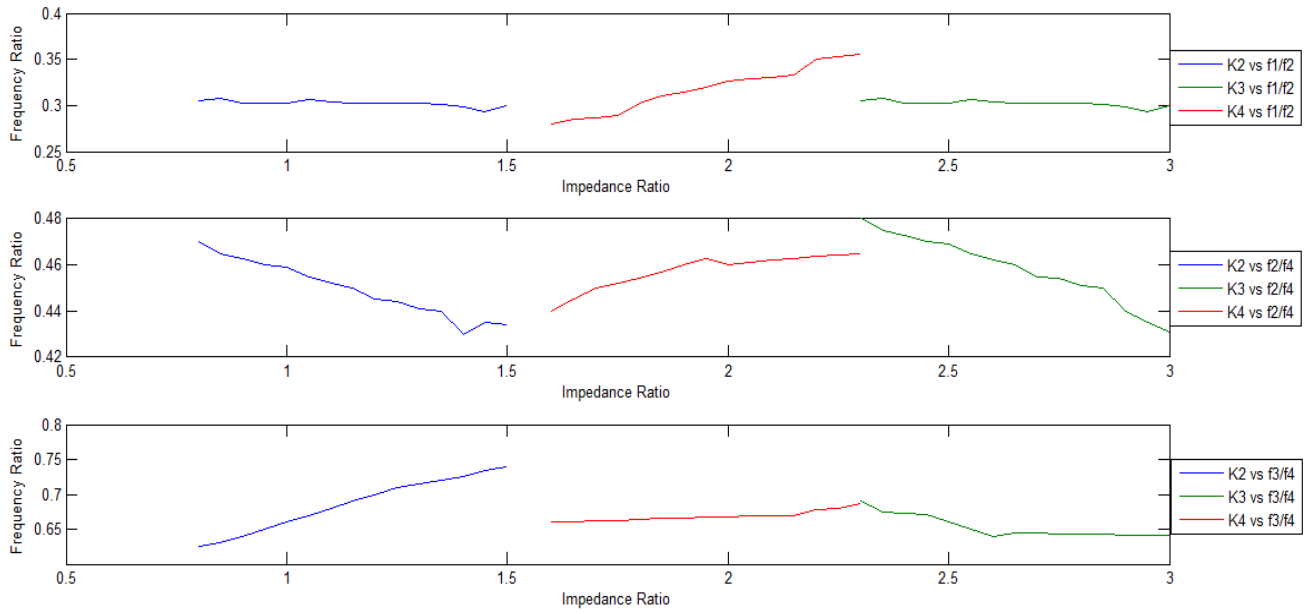

Fig. 2. Frequency characteristics of the proposed FSSIR with different impedance ratios K2, K3 and K4 (color online)

3. Antenna design

Fig. 3 depicts the suggested construction of the UWB antenna dimension (14 × 27.2) mm^2 with various slot sizes and shapes. This antenna is constructed from an FR-4 substrate. It has a permittivity of 4.3 and measures 1.5 mm in thickness. The material parameters window in CST Microwave Studio contains these substrate characteristics. The slotted patch and the reduced ground are made of copper with a thickness of 0.035 mm. Sections of SIR with four stages are referred to as feeders. Electrical lengths for four steps equal 3.75 with widths of 3, 1.5, 0.75, and 0.3525 with impedances of 50, 100, 200, and 400 Ohms.

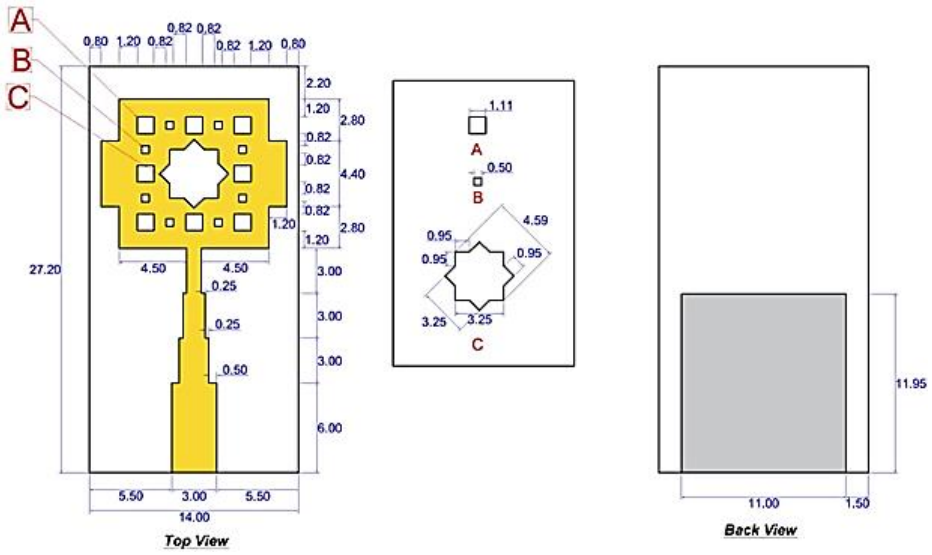

Fig. 3. The proposed UWB antenna from the top and the back sides (color online)

4. Results and discussion

UWB antenna is intended to span the frequency range of 2.92– 9.25 GHz under the finest match. The input reflection response by CST electromagnetic simulator is shown in Fig. 4. The input reflection values are 31, 30, and 32 dB at resonant frequencies of 3.3, 5.75, and 7.1 GHz, respectively. The impedance bandwidth is 6.33 GHz within -10 dB level.

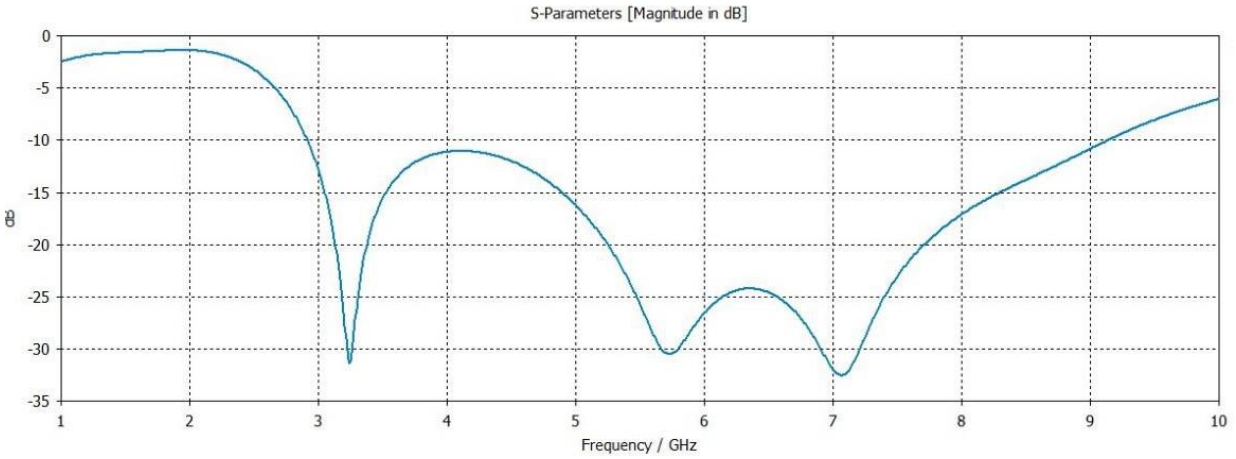

Fig. 4. Input reflection of the proposed UWB antenna (color online)

For 3D radiation patterns, at 3.2 GHz, the directivity gain is 1.68 dBi, 1.67 dBi at 5.8 GHz, and 1.56 dBi at 7 GHz are explained by Figs. 5, 6 and 7.

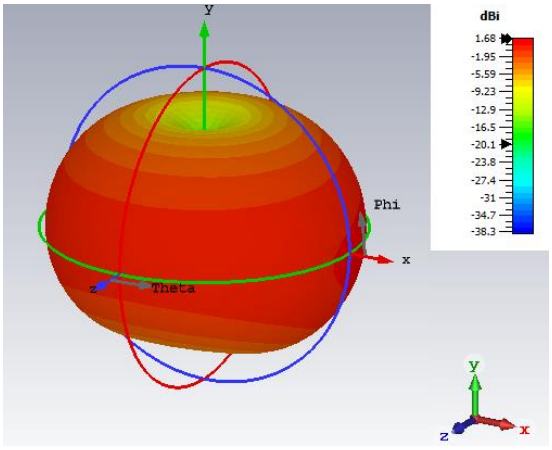

Fig. 5. 3D radiation pattern at 3.2 GHz (color online)

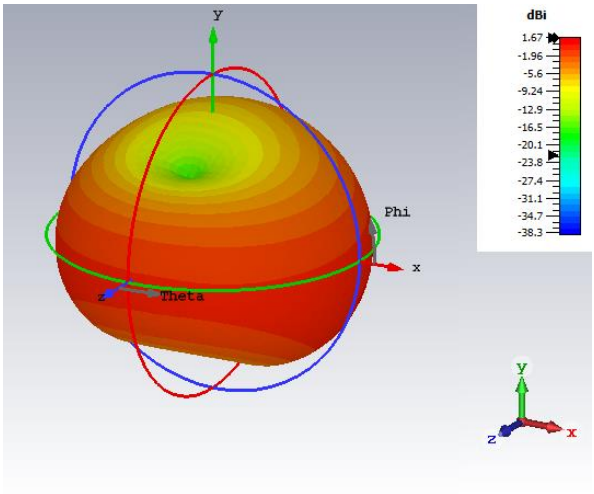

Fig. 6. 3D radiation pattern at 5.8 GHz (color online)

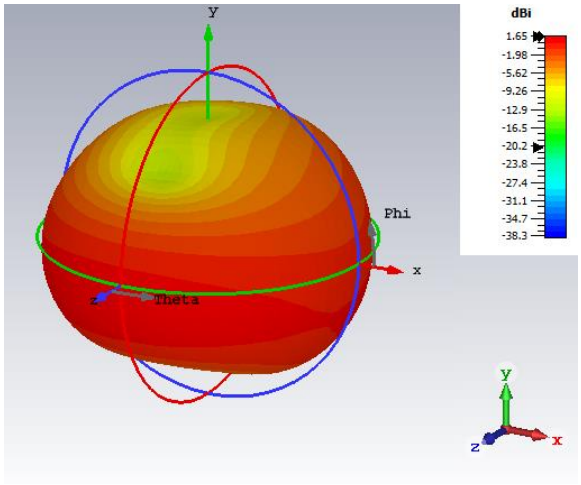

Fig. 7. 3D radiation pattern at 7 GHz (color online)

In the conductive areas for the projected UWB-based antenna, the simulated surface current distribution is presented. FSSIR feeder, slotted patch radiator bottom layer besides certain decreased ground plane margins are with an utmost current intensity of 5 A/m as seen in Fig. 8 that stands for in effect regions based on the highest current intensity.

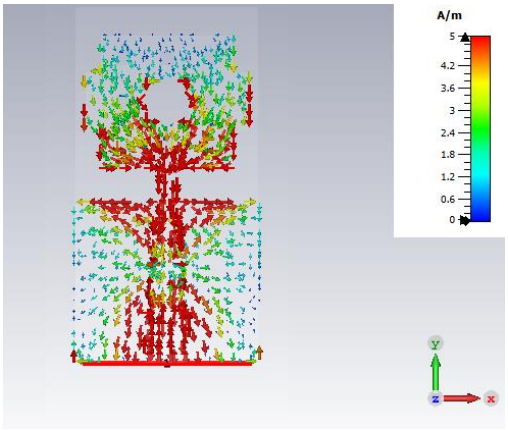

Fig. 8. A depiction showing how the antenna's surface current intensity is distributed (color online)

Within a frequency range of 3–7 GHz, the gain values are shown in Figs. 9 and 10 shows the radiation fields of the simulated far-distance patterns in the x-y, x-z, and y-z planes, respectively. As the x-y radiation patterns are perpendicular to the E plane and correspond with the H-plane of a vertically polarized antenna, the x-y radiation patterns are typical horizontal plane radiation patterns. Instead, the y-z plane and the E plane agree. So, the y-z patterns are vertical plane radiation patterns.

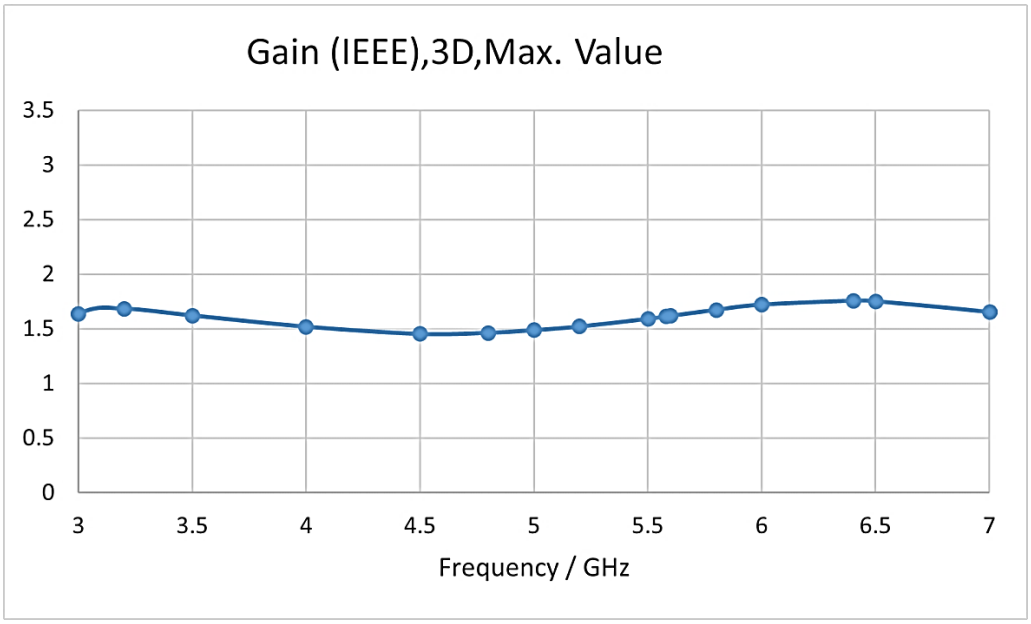

Fig. 9. UWB antenna gain based on FSSIR feeder

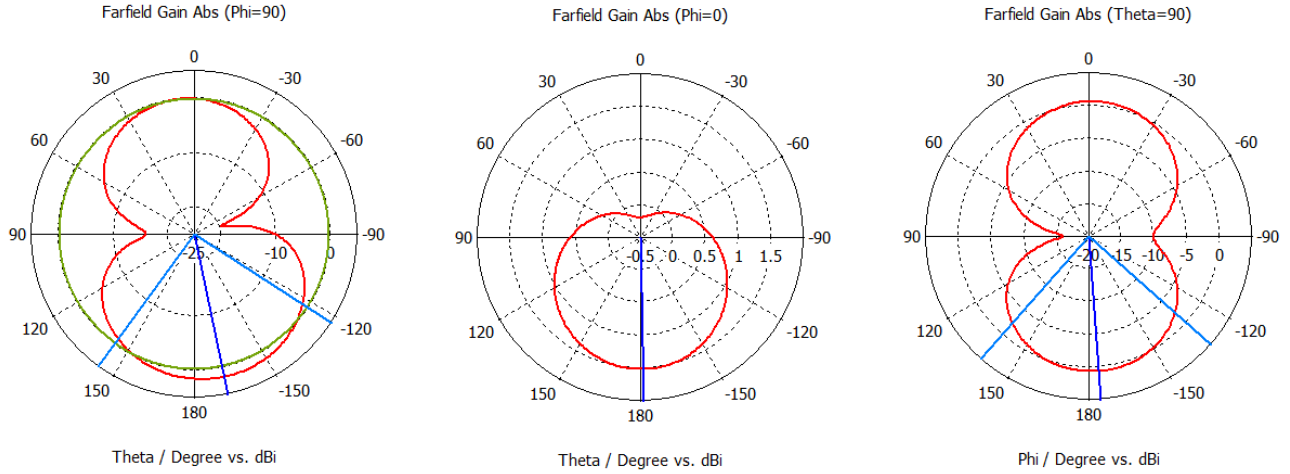

(a) 3.2GHz

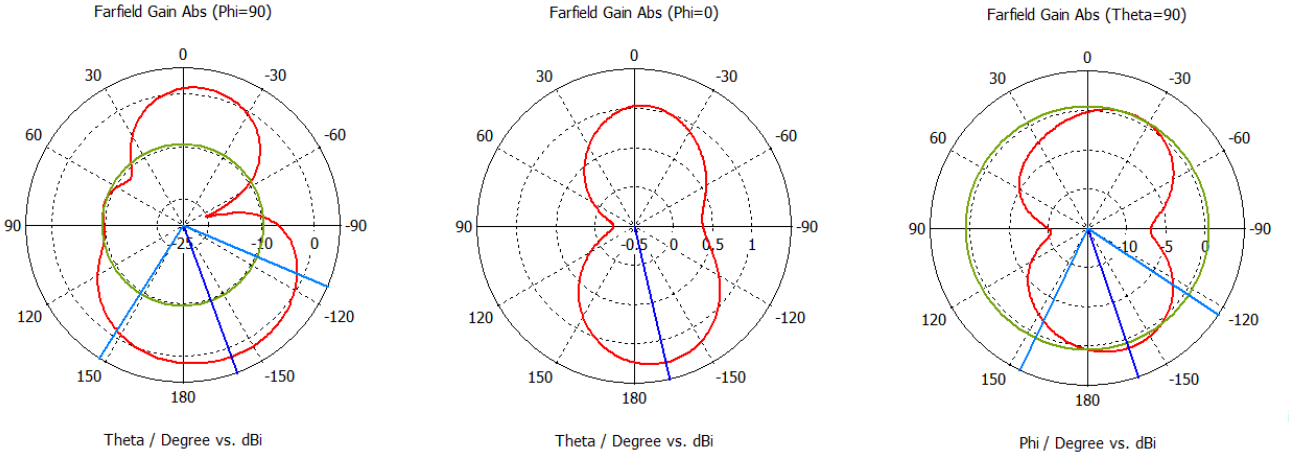

(b) 5.8GHz

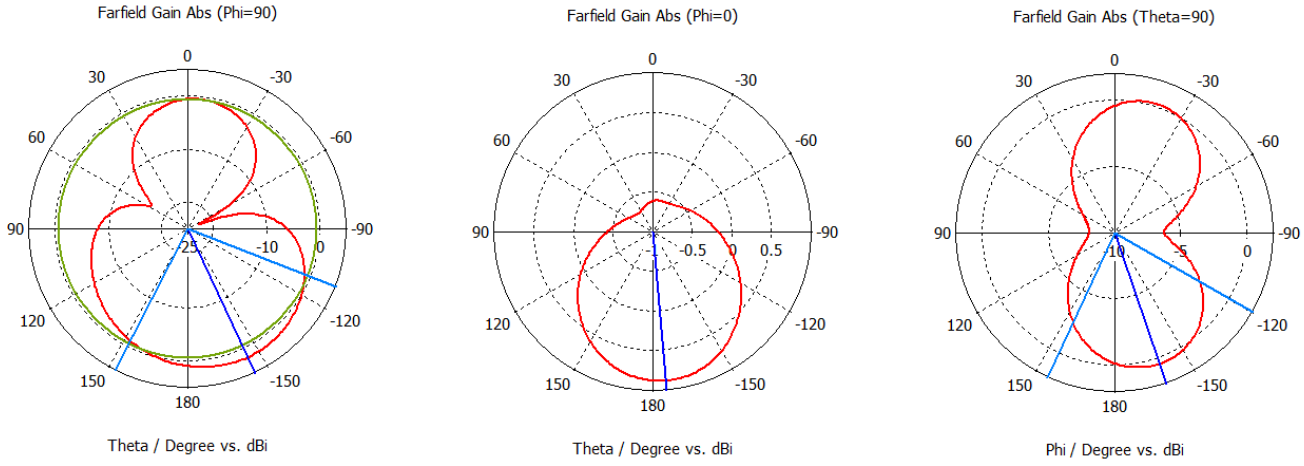

(c) 7 GHz

Fig. 10. Radiation patterns for projected UWB antenna @ (a) 3.2 GHz, (b) 5.8GHz and (c) 7GHz (color online)

Reported antennas in [13-22] have been compared with the UWB antenna in this article. Accordingly, the antenna in this article is designed to be as small as possible while maintaining a viable impedance bandwidth, as shown in Table 1. The proposed antenna in this research has very small dimensions, is cost-effective, has highest bandwidth, and can be easily manufactured in comparison to other antennas described in the literature.

Table 1. Comparative magnitudes among the diverse reported UWB antenna configurations with designed UWB antenna in this study

Ref.	***Dielectric Constant***	***Size (mm^3)***	***Bandwidth Range (GHz)***	Applications
[13]	4.3	30×35×1.6	7 – 9.9	UWB applications (X-band)
[14]	4.4	60×120×1.5	0.75-7.65	CR enabled wireless devices
[15]	2.2	63×56×0.34	28.5-27.4	5G applications
[16]	3.38	45×50×0.41	3-11.57	UWB/WiMAX applications
[17]	4.4	59.5×30×1.6	5.85-6.6	Industrial Scientific and Medical Band applications
[18]	2.8	50×55×1.6	2.73- 2.83	Applications of wideband and multiband frequency
[19]	4.9	50×40×1.6	1.62-2.7	Efficiency and Bandwidth Improvement
[20]	9.15	49×52×2.2	5.98-6.1	Applications for wireless and satellite communications
[21]	4.4	50×44.4×0.15	7.2-9.2	Wearable applications
[22]	4.4	60×80×1.6	7-8	C-band wireless communication
Proposed	4.3	14×27.2× 1.5	2.91-9.13	UWB applications

5. Parametrical study

Response to Input Reflection with Ground Plane Effect

According to Fig. 11, the same FSSIR feeder and a slotted patch radiator were used to explore the effect of different ground planes on the input reflection performance, as shown in this section. This is seen in Fig. 12, which depicts the ground plane's frequency response as it implements. For Step 4, the obtained UWB response is clearly visible, whereas the antenna displays a substantially very good impedance matching bandwidth in Step 4 than in other steps.

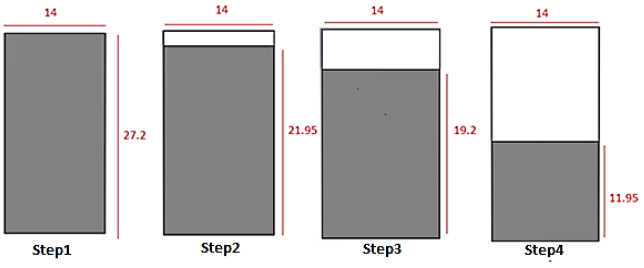

Fig. 11. Illustrating the various employed types of the ground plane

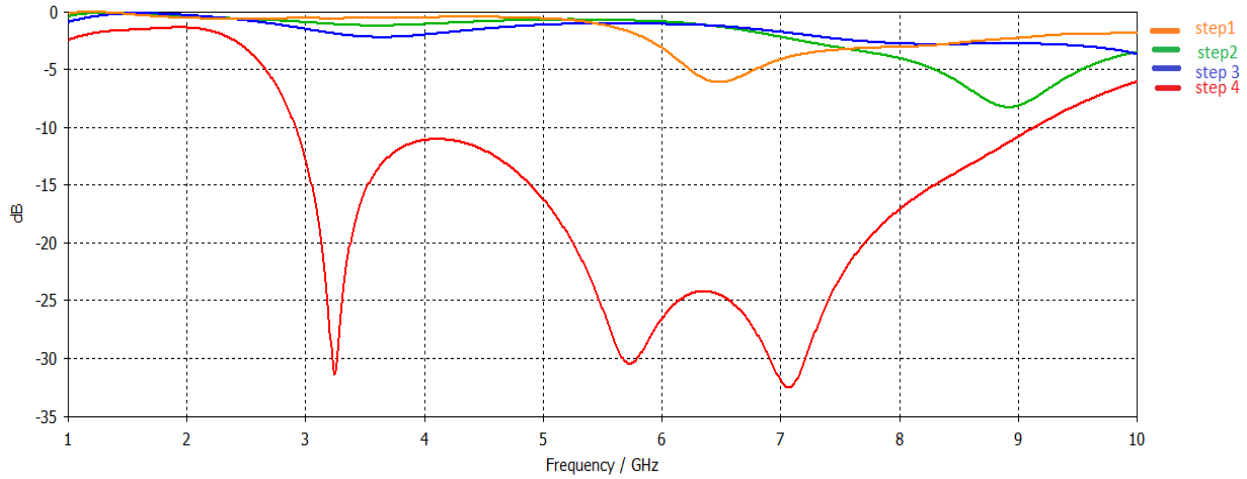

Fig. 12. Ground plane slotting impact on the input reflection response (color online)

Feeder effect on input reflection response

In this part, the impact of the different feeder types, as shown in Fig. 13, is thoroughly examined. A slotted patch radiator and a decreased ground plane have been used to analyze the distribution of input reflections. As a result, Fig. 14 shows that in Step1, a uniform impedance resonator (UIR) exhibits a poor frequency response. In comparison, the dual-band frequency response is clearly visible in Step 2 but with fair matching. Step3 shows the UWB response, but no notched band region has been detected. Step4 shows a higher impedance bandwidth and better return loss than the previous steps.

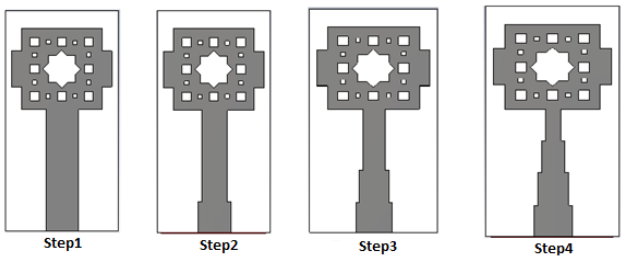

Fig. 13. Employing several steps in investigating antenna feeder, (a) UIR Feeder, (b) Bi-Sectional SIR Feeder, (c) Tri-Sectional SIR Feeder and (d) Four-stage SIR

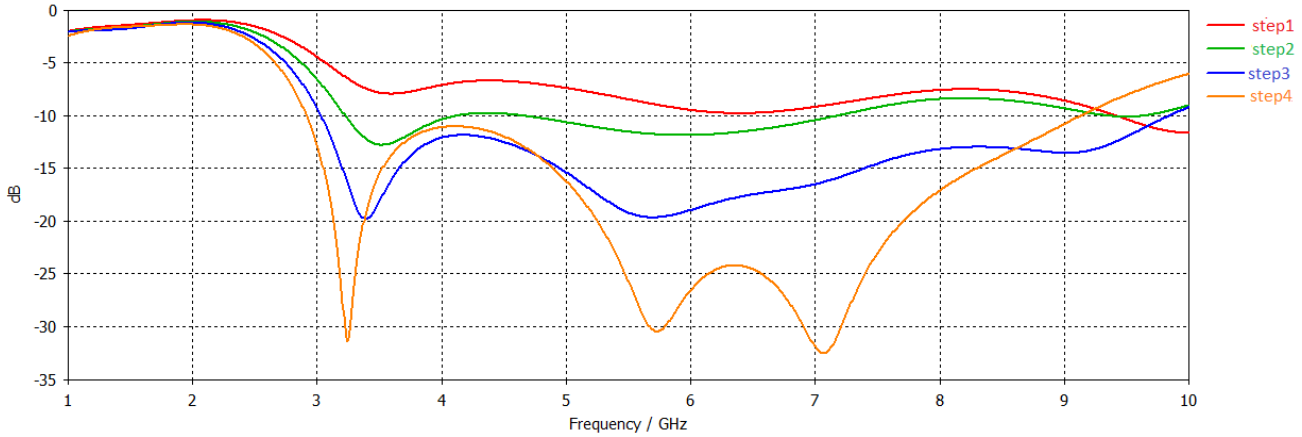

Fig. 14. Feeder cases impact on input reflection response (color online)

6. Fabrication and measurements

Including all design processes and optimization based on the CST simulator, the proposed UWB antenna has been prototyped using LPKF machines. An SMA coaxial connection, as seen in Fig. 15, was attached to the feedline end of the FR4 epoxy substratum. An Anritsu Vector Network Analyzer is used for the S11 measurement experimentation as in Fig. 16. The measured S11 result is depicted in Fig. 17 that is in reasonable agreement with the simulated result, with acceptable fluctuations owing to soldering, Cu losses, substrate losses, connecting cables, and the measuring environment.

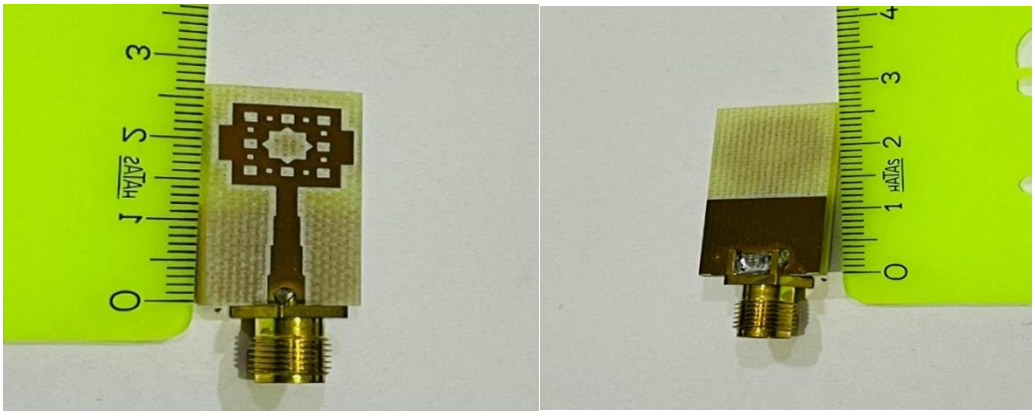

(a) (b)

Fig. 15. Prototype shots for the projected UWB antenna: (a) Top View and (b) Bottom View (color online)

Fig. 16. Measurement setup shot (color online)

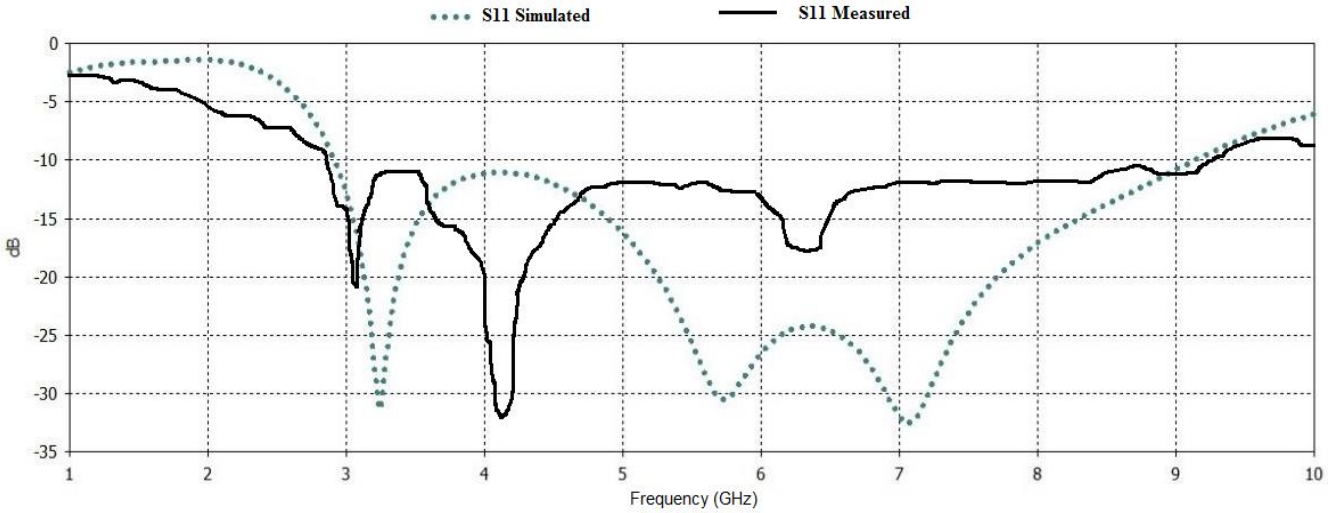

Fig. 17. The measured and simulated S11 responses for the designed UWB antenna based on the FSSIR feeder within 1-10 GHz frequency sweeping range

7. Conclusion

In this study, a new miniaturized UWB antenna using an FSSIR feeder has been firstly presented for the demands of modern wireless communities. To overcome some technical limitations of the employed substrate and UWB antenna design, a slotted patch resonator and reduced ground plane were employed to create and simulate this antenna using FR-4 substrate. The slotted patch and the reduced ground are made of copper with a thickness of 0.035 mm. Sections of SIR with four stages are referred to as feeders. Electrical lengths for four steps equal 3.75 with widths of 3, 1.5, 0.75, and 0.3525 with impedances of 50, 100, 200, and 400 Ohms. The simulated

S11 scattering response indicated that UWB bandwidth is within the 2.91 – 9.13 GHz frequency range with a gain better than 1.5 dBi and acceptable input reflection. The simulated S11 consequences are in good agreement with the measurements. Compared to several documented UWB-based antennas in the literature, the suggested antenna has more compactness and higher bandwidth.

Acknowledgment

Special thanks to research assistant "Sedat Kilinc" of Istanbul University-Cerrahpasa RF Lab for his support in measurements.

References

[1] W. Tang, M. Z. Chen, J. Y. Dai, Y. Zeng, X. Zhao, S. Jin, Q. Cheng, T. J. Cui, IEEE Wireless Communications **27**(2), 180 (2020).
[2] Z. Ul, Z. Ullah, Int. J. Adv. Comput. Sci. Appl. **8**(10), 379 (2017).
[3] S. F. Wang, Y. Z. Xie, IEEE Transactions on Antennas and Propagation **70**(8), 7142 (2022).
[4] Y. Zehforoosh, M. Mohammadifar, A. H. Mohammadifar, S. R. Ebadzadeh, J. Microwaves Optoelectron. Electromagn. Appl **16**(3), 765 (2017).
[5] T. K. Saha, C. Goodbody, T. Karacolak, P. K. Sekhar, Microw. Opt. Technol. Lett. **61**(1), 182 (2019).
[6] R. Soni, R. Gupta, D. Sen, Int. J. Recent Technol. Eng. **8**(5), 4517 (2020).
[7] A. K. Dwivedi, B. Mishra, V. Singh, P. N. Tripathi, A. K. Singh, Electr. Control Commun. Eng. **16**(1), 15 (2020).
[8] D. Venkatachalam, M. Govindasamy, Appl. Math. Inf. Sci. **13**(1), 73 (2019).
[9] Rupali, R. Rajni, Int. J. Comput. Sci. Netw. no. September, 54 (2018).
[10] F. Cheng, X. Q. Lin, Y. Jiang, K. J. Song, Y. Fan, Prog. Electromagn. Res. Lett. **44**, 101 (2014).
[11] Z. H. Ma, Y. F. Jiang, Micromachines **11**(9), 1 (2020).
[12] H. W. Xie, K. Zhou, C. X. Zhou, W. Wu, Int. J. RF Microw. Comput. Eng. **30**(4), 1 (2020).
[13] Q. M. Hamza, S. M. Nabil, M. Hassan, International Symposium on Advanced Electrical and Communication Technologies (ISAECT) **4**(2), 78 (2019).
[14] R. Hussain, M. S. Sharawi, A. Shamim, IEEE Transactions on Antennas and Propagation **66**(2), 978 (2018).
[15] K. A. Fante, M. T. Gemeda, Int. J. Electr. Comput. Eng. **11**(3), 2238 (2021).
[16] Y. M. Mohamed, H. Abdallah, E. EI-Hennawy, IEEE Access **7**, 36010 (2019).
[17] R. Sanmugasundaram, D. Dileepan, S. Natarajan, International Journal of Engineering and Technology **7**(4), 2525 (2018).
[18] D. Rusdiyanto, C. Apriono, D. W. Astuti, M. Muslim, Synergy **25**(2), 153 (2021).
[19] A. Mithari, U. Patil, Int. Res. J. Eng. Technol. **3**(4), 2696 (2016).
[20] M. K. Abdulhameed, M. S. M. Isa, I. M. Ibrahim, M. K. Mohsen, S. R. Hashim, M. L. Attiah, J. Adv. Res. Dyn. Control Syst. **10**(4) Special Issue, 661 (2018).
[21] D. Negi, R. Khanna, J. Kaur, International Journal of Microwave and Wireless Technologies **11**(8), 806 (2019).
[22] A. H. A. Al-Shaheen, ARPN J. Eng. Appl. Sci. **14**(6), 1249 (2019).

*Corresponding email: yaqeen@esraa.edu.iq, yakeen_sbah@yahoo.com